EM Implosion Memos

Memo 39

February 2010

Investigation of various switch configurations

Prashanth Kumar, Serhat Altunc, Carl E. Baum, Christos G. Christodoulou and Edl Schamiloglu
University of New Mexico
Department of Electrical and Computer Engineering
Albuquerque, NM 87131

Abstract

Four switch designs are explored using numerical simulations. These configurations are then compared based on the focal impulse amplitude, beam width and ease-of-fabrication.

1 Introduction

The possiblity of using the switch structure to launch *and* guide the spherical TEM wave gives rise to many alternative launching configurations [1]. The choice of a configuration is dictated by its conceptual simplicity and practical viability. One configuration, the vertical bicone switch, was explored in [2]. This paper investigates other possible switch structures, specifically,

- Four feed arms with switch cones,
- Truncated four feed arms with switch cones,
- Slanted bicones,
- Slanted four-cones.

The focal impulse amplitude, beam width and ease-of-fabrication are used to evaluate the advantages of each of these structures. Numerical simulations are used to compare the focal impulse response and spot size for each of the designs.

2 Setup

2.1 Structure Visualization

2.1.1 Four feed arms (without switch cones) [4FA]

Figure 2.1 shows the perspective view of the 4FA and reflector system. The excitation is applied between a 2 mm gap in the feed arms. The first focal point is approximately 0.1 mm from the center of the excitation. This configuration represents a conceptual design. It does not contain any switch cones and is considered for the purposes of comparison only.

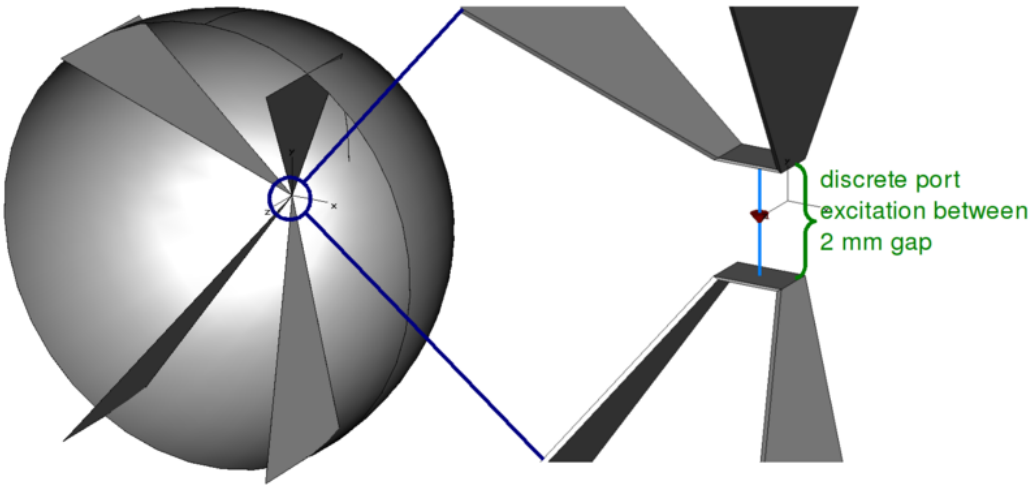

Figure 2.1: Perspective view of four feed arms and reflector; "Zoomed-in" view showing discrete port excitation.

2.1.2 Four feed arms with switch cones [4FASC]

Figure 2.2 shows the perspective view of the 4FASC and the reflector. The side view and geometrical details of the switch cones and loft connections are shown in Fig. 2.3.

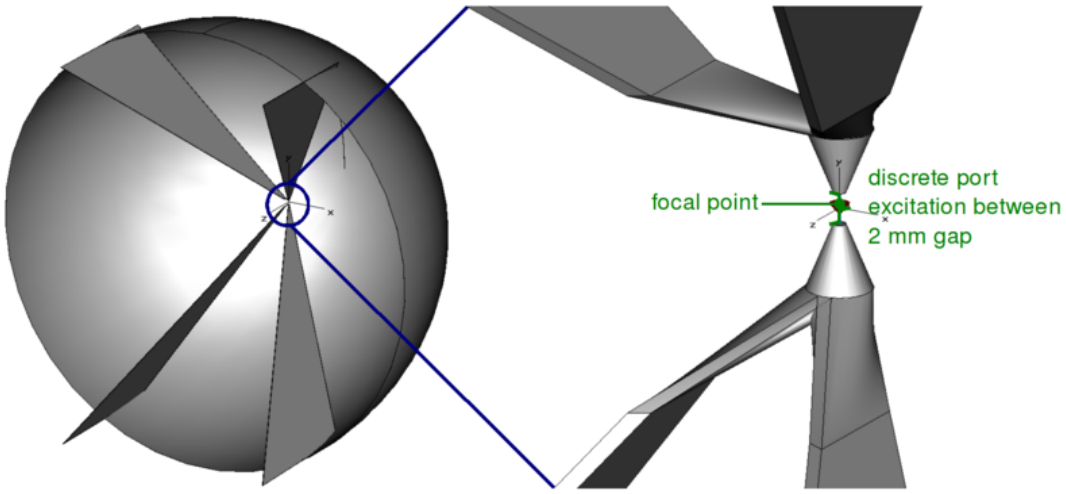

Figure 2.2: Perspective view of four feed arms with switch cones and reflector; "Zoomed-in" view, around first focal point, showing discrete port excitation.

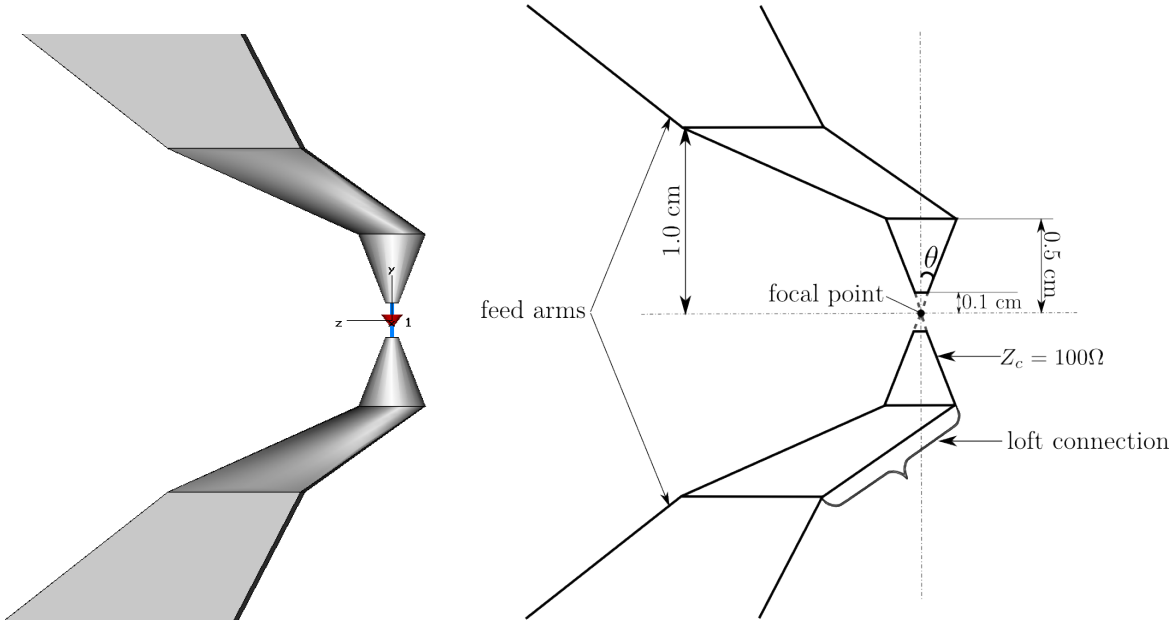

(a) "Zoomed-in" side view of the feed arms and switch cones.

(b) Geometric details of feed arms and switch cones.

Figure 2.3: "Zoomed-in" side view and geometric details of feed arms and switch cones.

The loft connections were made between the circular switch cone base, $y = 0.5$ cm, and the flat face of the feed arm, $y = 1.0$ cm, as shown in Fig. 2.3(b).

2.1.3 Truncated four feed arms with switch cones [T4FASC]

Figure 2.4 shows the perspective view of the T4FASC and the reflector. The setup is almost identical to Fig. 2.2 except that the feed arms are (arbitrarily) truncated at $y = 10$ cm as shown in Fig. 2.5. The details of the switch geometry are exactly the same as Fig. 2.3.

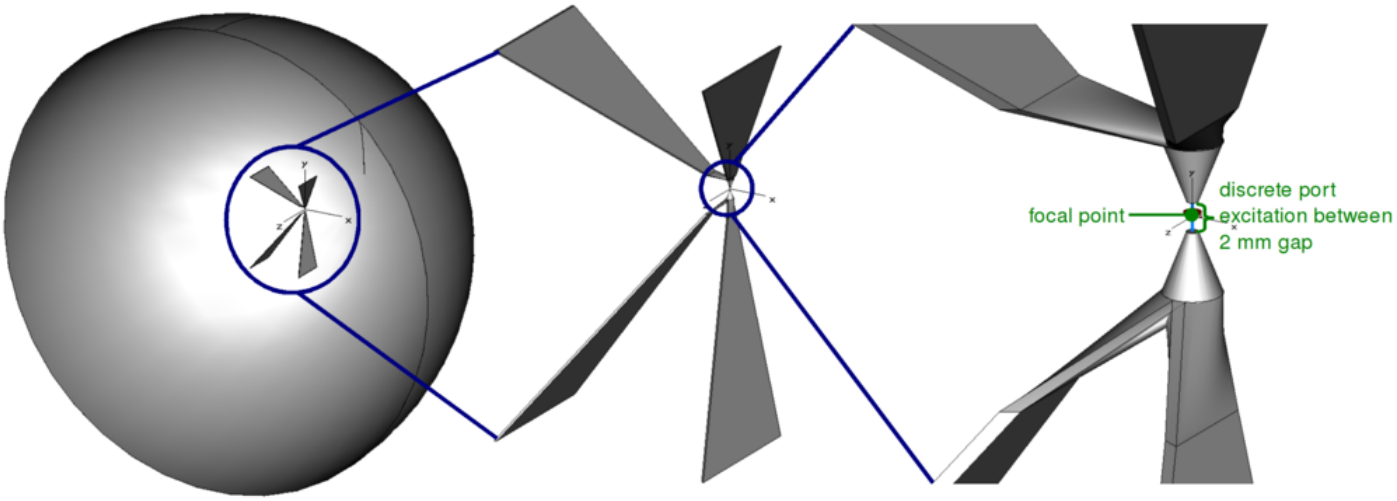

Figure 2.4: Perspective view of truncated four feed arms with switch cones and reflector; "Zoomed-in" view, around first focal point, showing discrete port excitation.

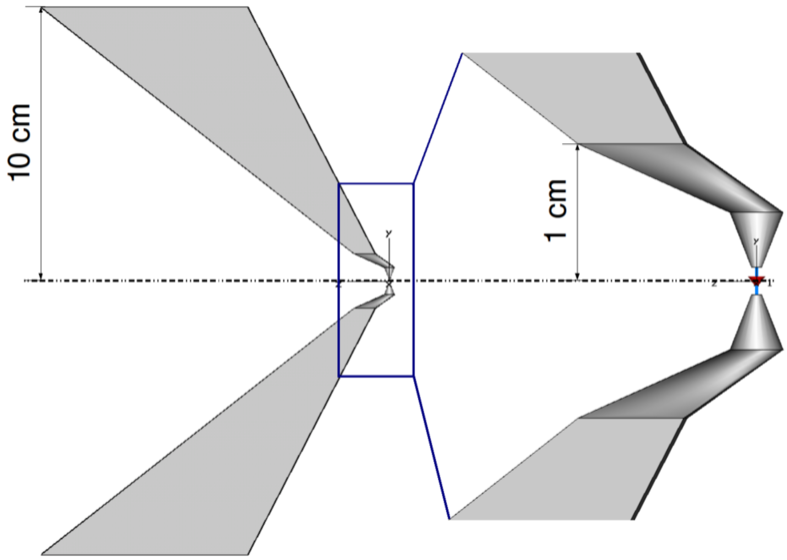

Figure 2.5: Side view of truncated four feed arms with switch cones and reflector. Feed arms are truncated at $y = 10$ cm.

2.1.4 Truncated four feed arms with slanted switch cones [T4FASSC]

Figure 2.6 shows the perspective view of the T4FASSC and reflector system. The side view and geometrical details of the slanted cones and loft connections are shown in Fig. 2.7.

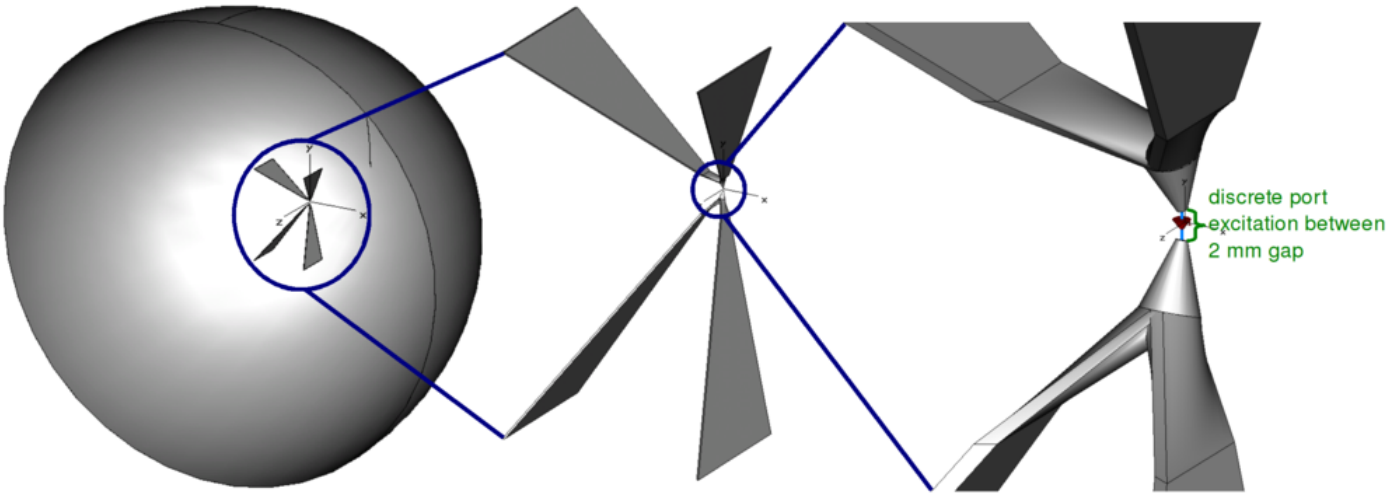

Figure 2.6: Perspective view of four feed arms with slanted switch cones and reflector; "Zoomed-in" perspective view of the slanted switch cone configuration.

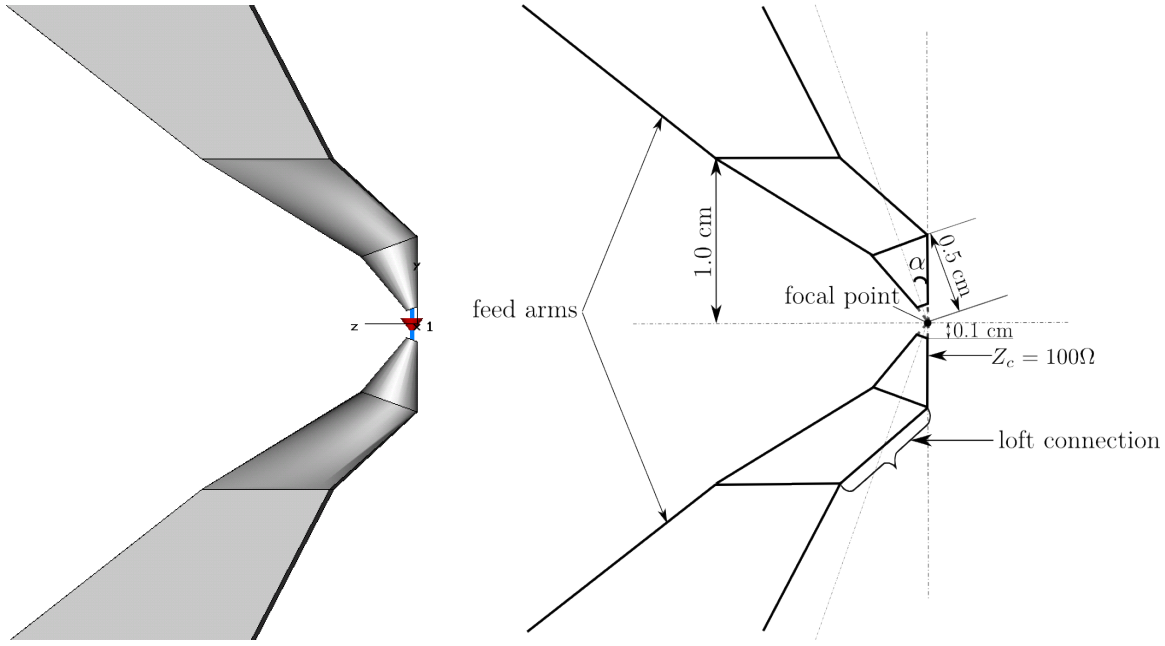

(a) "Zoomed-in" side view of the feed arms and slanted switch cones.

(b) Geometric details of the feed arms, loft connections and slanted switch cones.

Figure 2.7: "Zoomed-in" side view and geometric details of the feed arms and slanted switch cones.

The (virtual) apex of the cones meet at the first focal point. The half-angle, $\alpha = 20.04°$, of the cones is calculated in [3]. The setup is very similar to the configuration in [1]. The lengths of the loft connection, $y = 1.0$ cm, and truncated feed arm, $y = 10.0$ cm, are shown in Fig. 2.8. A discrete port excitation is applied between a 2 mm gap in the two cones. The excitation does *not* pass through the first focal point due to the inclination of the cones.

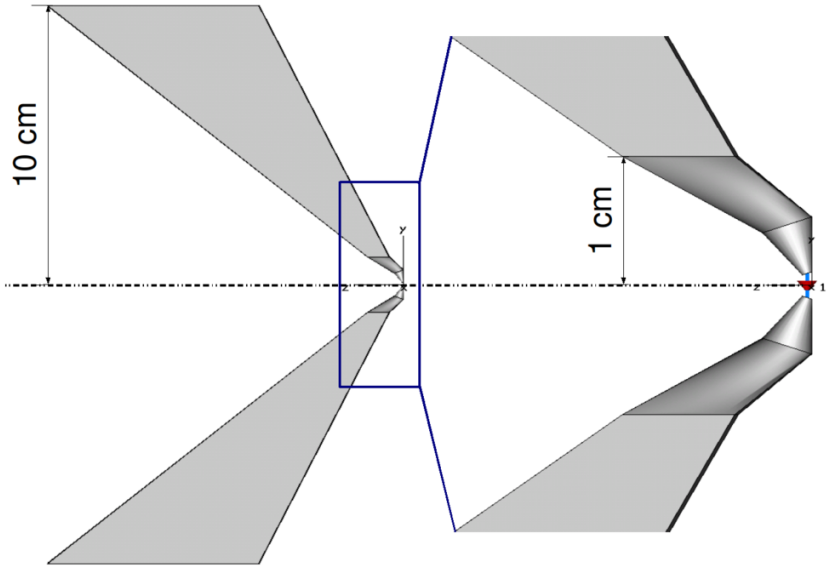

Figure 2.8: Side view of feed arms with slanted cone source; "Zoomed-in" side view, around first focal point, showing slanted cones and loft connections.

2.1.5 Slanted bicone feed arms [S2CFA]

Figure 2.9 shows the perspective view of the S2CFA and reflector system.

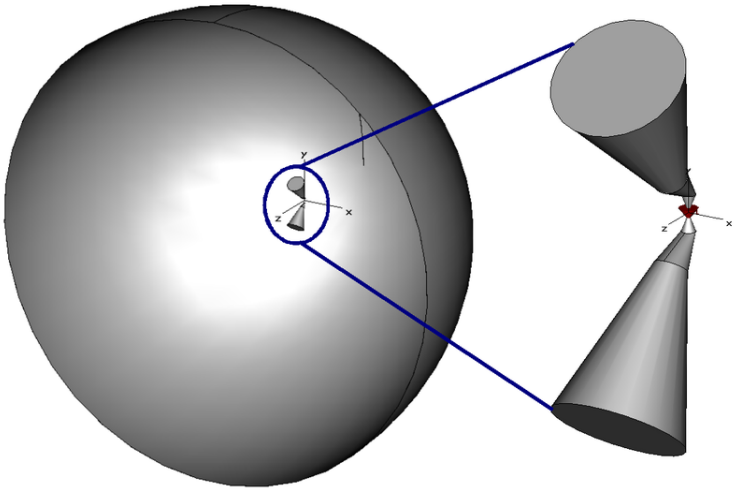

Figure 2.9: Perspective view of the slanted bicone switch and reflector system; "Zoomed-in" perspective view of the slanted switch cone configuration.

The slanted cones can be considered analogous to the feed arms in the two feed-arm system. The cones are inclined at the same angle as the feed arms, i.e., tan(4/3) rad. The side view of the cones is shown in Fig. 2.10. Details of the switch geometry are shown in Fig. 2.11.

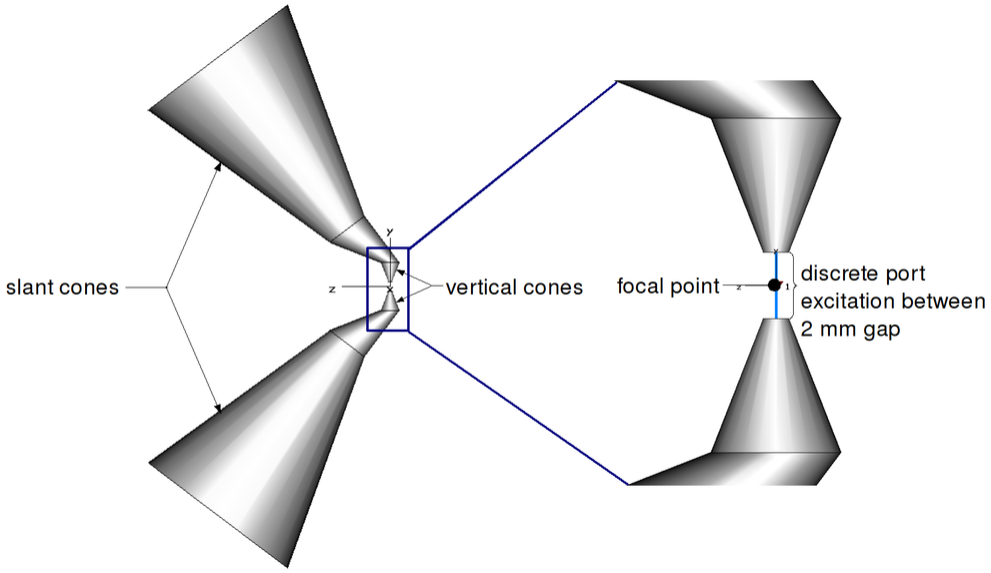

Figure 2.10: Side view of the slanted switch cones with vertical bicone source; "Zoomed-in" side view, around first focal point, showing discrete port excitation between the vertical cones.

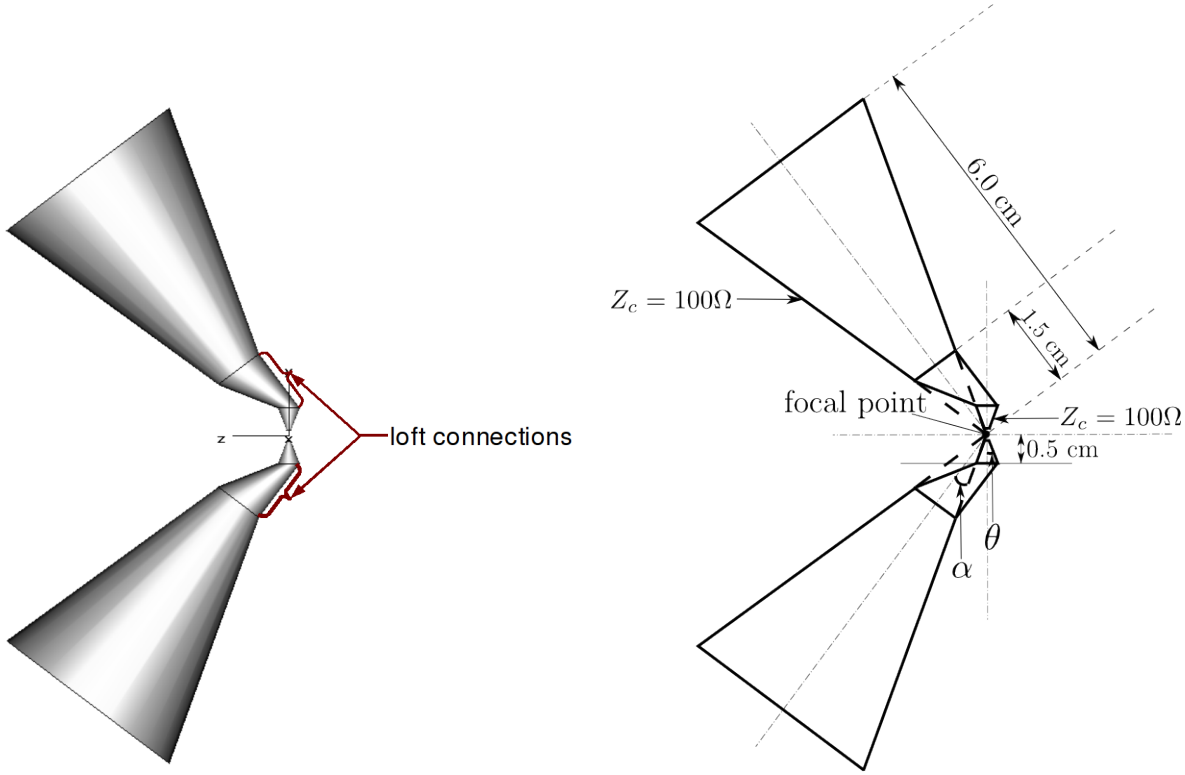

(a) "Zoomed-in" side view of the feed arms and switch cones.

(b) Geometric details of the feed arms and switch cones.

Figure 2.11: "Zoomed-in" side view and geometrical details of the feed arms and switch cones.

The slanted cones serve to guide the outgoing spherical TEM waves. The height of the slanted cones, from the apex to the base, is 6.0 cm $> ct_\delta = 3.0$ cm. The impedance of the slanted and vertical cones, $Z_c = 100\ \Omega$, is chosen as it leads to a practically reasonable geometry. The half-angle of the vertical cones, θ, is 21.37° [4]. The half-angle of the slant cones, α, is calculated using the stereographic projection formula from [3], where $\beta = \tan(4/3)$. Hence,

$$\alpha = \arcsin\left(\sin\beta\left[\cosh\frac{\pi Z_c}{Z_0}\right]^{-1}\right) = \arcsin\left(\sin\beta\left[\cosh\frac{\pi\ 200\Omega}{377\Omega}\right]^{-1}\right) = 16.97° \tag{2.1}$$

It is not immediately obvious which orientation of the slanted cones would yield the maximum focal impulse electric field. For comparison, a mirrored configuration (MS2CFA) was also simulated as shown in Fig. 2.12.

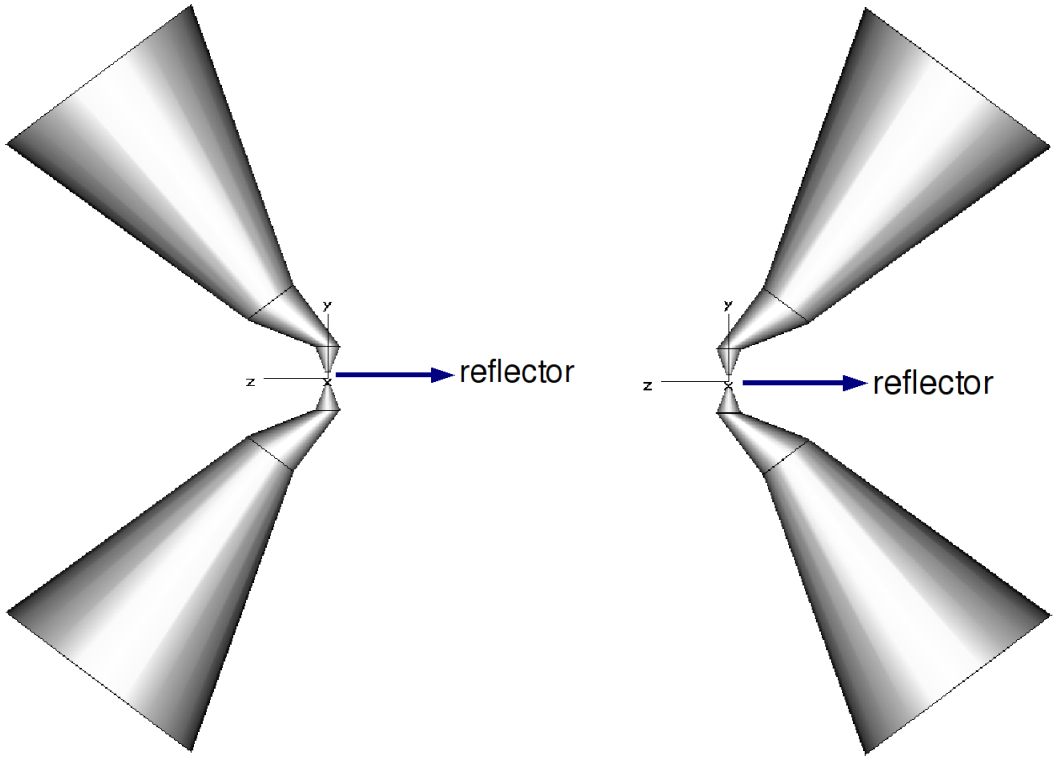

(a) Side view of slanted bicone switch.

(b) Side view of mirrored slanted bicone switch.

Figure 2.12: Slanted bicone switch and mirror configurations.

2.1.6 Slanted four-cone feed arms [S4CFA]

Figure 2.13 shows the perspective view of the S4CFA and reflector system.

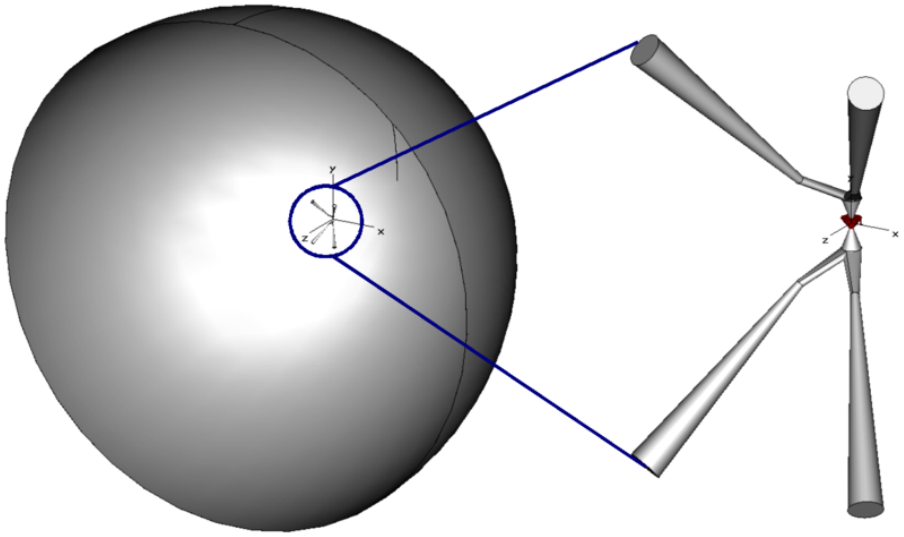

Figure 2.13: Perspective view of slanted switch cones and reflector; "Zoomed-in" perspective view of slanted switch cone configuration.

The slanted four cones can be considered analogous to the feed arms in the 4FA system. The cones are inclined at the same angle as the feed arms, i.e., tan(4/3) rad. The side view of the slanted switch cones is shown in Fig. 2.14. Details of the switch geometry are shown in Fig. 2.15.

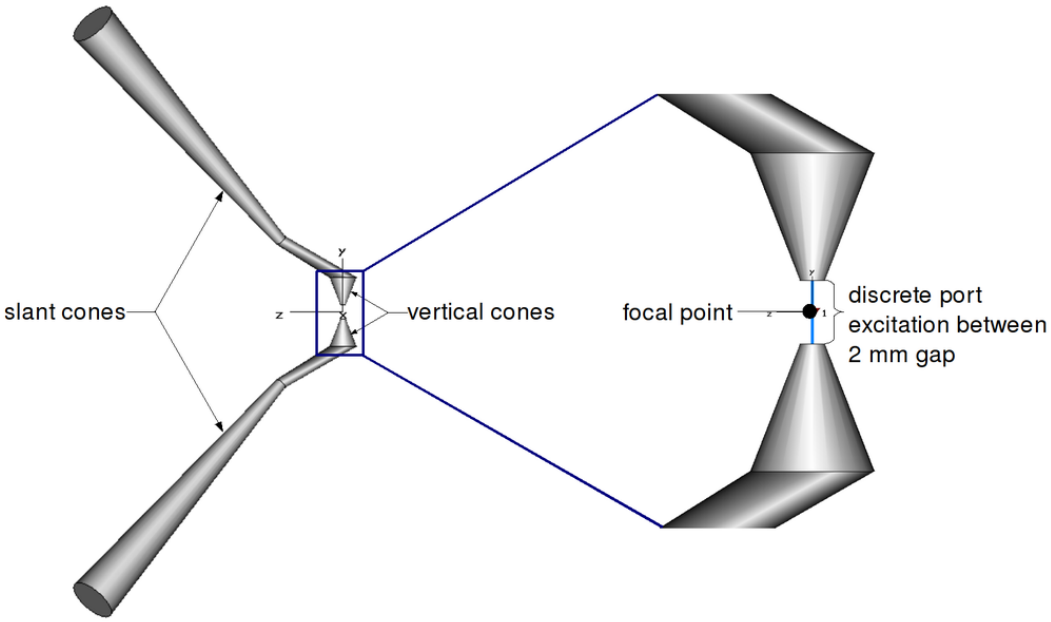

Figure 2.14: Side view of the slanted four-cone switch with a vertical bicone source; "Zoomed-in" side view, around first focal point, showing the discrete port excitation between vertical cones.

The design is almost identical to the slanted bicone switch. The impedance of the vertical cones is $Z_c = 100\ \Omega$. The impedance of the slant cones, $Z_c = 200\ \Omega$, is the same as the feed arms in the four feed-arm PSIRA. These impedance values lead to a practically reasonable geometry. The half-angle of the slant cones, α, is calculated using the stereographic projection formula from [3], where $\beta = \tan(4/3)$. Hence,

$$\alpha = \arcsin\left(\sin\beta\left[\cosh\frac{\pi Z_c}{Z_0}\right]^{-1}\right) = \arcsin\left(\sin\beta\left[\cosh\frac{\pi\ 400\Omega}{377\Omega}\right]^{-1}\right) = 3.27^\circ \tag{2.2}$$

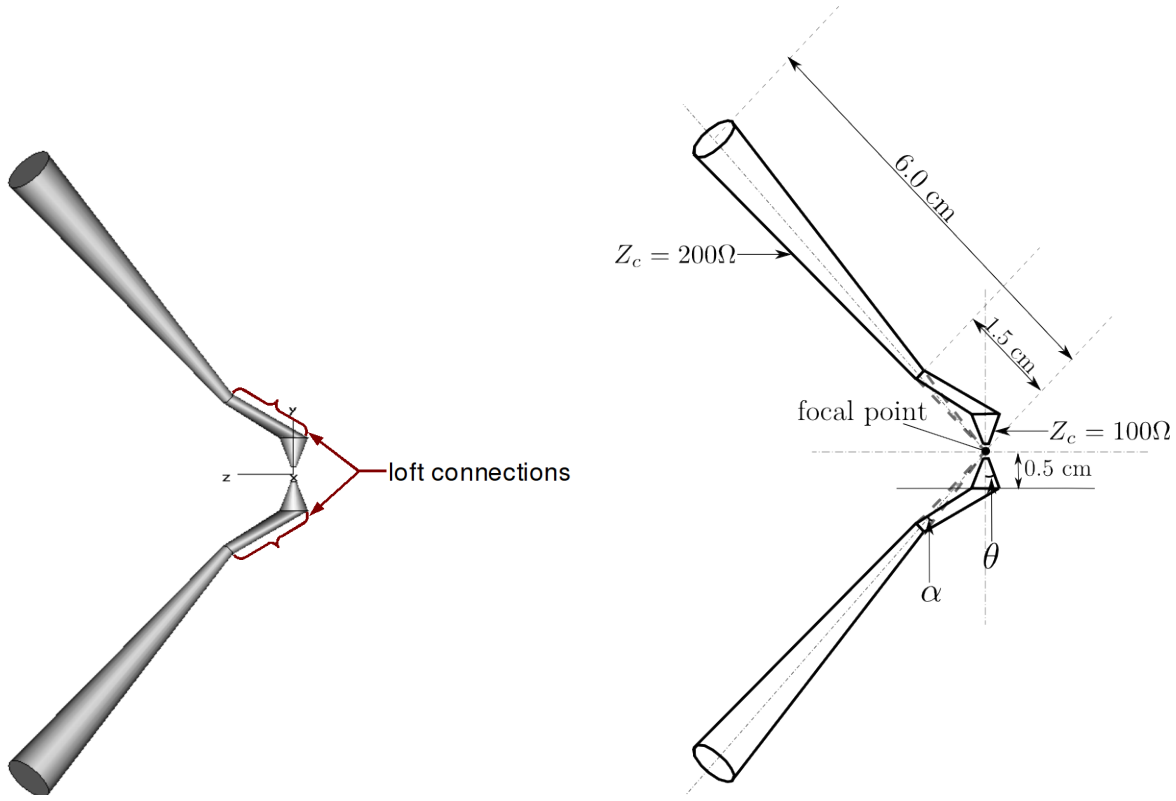

(a) "Zoomed-in" side view of the feed arms and four-cone switch.

(b) Geometric details of the feed arms and four-cone switch.

Figure 2.15: "Zoomed-in" side view and geometrical details of the feed arms and four-cone switch.

As in the case of the S2CFA, it is not immediately obvious which orientation of the slanted cones would yield the maximum focal impulse electric field. For comparison, a mirrored configuration (MS4CFA) was also simulated, as shown in Fig. 2.16.

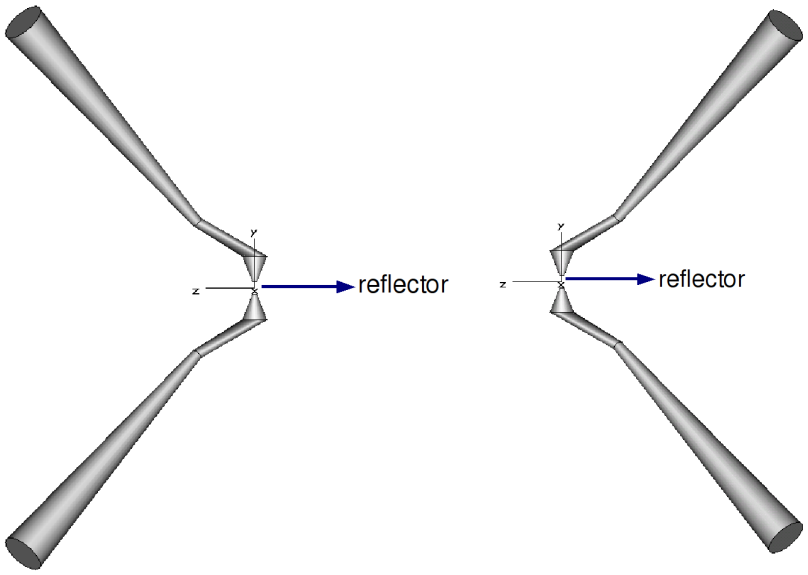

(a) Side view of slanted four-cone switch. (b) Side view of mirrored slanted four-cone switch.

Figure 2.16: Slanted four-cone switch and mirror configurations.

2.2 Notes

In the 4FASC, T4FASC, S2CFA and S4CFA configurations the following similarities are observed,

- The excitation is applied between two vertical cones. One notes the following features about these cones,
  - The impedance of each cone is $Z_c = 100\ \Omega$ (bicone impedance $= 2Z_c$), i.e., the half-angle of the cones is, $\theta = 21.37°$ [2].
  - The height of each cone is $h = 0.5$ cm. $h < ct_\delta = 3.0$ cm, so that the wave is guided by the cones, loft connections, and the guiding structures. For the 4FASC and the T4FASC, the guiding strutures are feed arms, while for the S2CFA and S4CFA, the guiding structures are slanted cones.
  - The geometric center of the switch cones (virtual apex) is the first focal point.
  - A discrete port excitation is applied between a 2 mm gap in the cones.

  In the final design, these vertical cones will be enclosed in the hydrogen chamber and pressure vessel.
- The loft connection is of arbitrary length. However, the loft connection cannot be too long as this would perturb the spherical wave originating from the center; too short a loft connection would not lead to a smooth transition between the switch cones and the feed arms.

Regarding the S2CFA and S4CFA designs, one notes the following,

- The slanted cones "shadow" a smaller area on the reflector, compared to the cones in the vertical bicone switch [2].

- The loft connection transitions between two circular cross sections, i.e., from the switch cones to the slanted cones, as shown in Fig. 2.11 and Fig. 2.15. This is easier to fabricate than the loft connections of the 4FASC and T4FASC structures, where the transition is between the circular base of the switch cones and the flat face of the feed arms.

The electric field probe placements and orientations are identical to those in [2].

2.3 Important CST/Simulation Parameters

Domain	Time
Excitation	Discrete
Input	Ramp rising step with 100 ps rise time
Excitation voltage	1 V
Frequency range	0−10 GHz
LPW	10

3 Results

The peak focal impulse amplitude ($E_{\max}$) and beam width (spot size) for the launching configurations presented above are summarized in Table 1. The table also presents the vertical bicone switch (VBCS) results from [2] where VBCS-X is a switch with Z_c = 2X Ω. Options worthy of consideration, based on the focal impulse amplitude, beam width and ease-of-fabrication, are highlighted. The 4FA represents a hypothetical case and is therefore not considered/highlighted. The plots of the focal waveform and beam width for all configurations are provided in the appendix.

Table 1: Peak focal impulse amplitude and beam width for various switch configurations.

Configuration	$E_{\max}$ (V/m)	Spot size (cm)
VBCS-50	8.117	3.737
VBCS-75	6.727	3.894
VBCS-100	5.619	4.065
VBCS-125	4.708	4.304
VBCS-150	4.057	4.414
VBCS-200	3.144	4.455
4FA	6.677	3.288
4FASC	6.363	3.546
T4FASC	7.217	3.889
T4FASSC	7.379	3.907
S2CFA	6.095	3.715
MS2CFA	2.774	> 6.000
S4CFA	5.114	3.39
MS4CFA	2.343	> 6.000

4 Discussion

4.1 Easiest to fabricate

The VBCS-75 and VBCS-100 designs yield a reasonable focal impulse amplitude compared to the 4FA case. These configurations also yield a very high $E_{\max}$, compared to the other VBCSs, for fixed input power [2]. However, the beam width is larger compared to the 4FASC case, for e.g. for VBCS-100 the spot size is larger by approximately 0.5 cm. One advantage of the VBCS is that the prepulse is shorter and smaller than the 4FA and 4FASC designs, which is desirable [2]. Of all the configurations in Table 1, the VBCS is the easiest to fabricate.

The VBCS will ultimately be immersed in the pressure vessel dielectric. Consequently, the impedance of the cones in the dielectric will be reduced to $Z_c/\sqrt{\epsilon_{rp}}$, where ϵ_{rp} is the relative permittivity of the pressure vessel. This in turn will increase the half-angle of the cones inside the dielectric. The VBCS-50 was not considered as it may pose problems at high voltages, such as arcing, due to the very large half-angles inside the pressure vessel and therefore would not be practical.

4.2 Smallest spot size

The 4FASC, which may be considered as the simplest extension to the 4FA, yields the smallest spot size of the highlighted configurations. However, the focal impulse amplitude is smaller than the VBCS-75, T4FASC and T4FASSC. As seen in Fig. 5.1(c), the focal impulse waveform for the 4FASC is similar to the 4FA case, i.e., the pre-pulse, impulse and post-pulse look very similar. This configuration is therefore most useful if the primary objective is to obtain a small spot size, even if $E_{\max}$ is reduced as a consequence.

4.3 Largest impulse amplitude

The truncated four feed-arm configurations, T4FASC and T4FASSC, yield the highest impulse amplitudes compared to other highlighted configurations in the table. This comes at the cost of an increased spot size, though this increase is $\lessapprox 0.4$ cm, compared to, say, the 4FASC. An additional advantage of the truncated feed arm designs is the dispersion of the prepulse as observed in Fig. 5.2(a) and Fig. 5.2(c), which is desirable. Note that the T4FASSC is more difficult to fabricate, than the T4FASC, due to the inclination of the switch cones.

The slanted cone configurations, S2CFA, MS2CFA, S4CFA, and MS4CFA, are designed for a bicone impedance of 200 Ω. For this impedance, the results in Table 1 indicate a smaller $E_{\max}$ and a larger spot size than the highlighted structures. This is undesirable. The cone impedances in the S2CFA and S4CFA may be varied, as done for the VBCS in [2]. Different cone impedances for the S2CFA and S4CFA may yield better results. However, the S2CFA and S4CFA are more complicated, and the simplicity of the highlighted structures in the table are more preferable.

5 Conclusions

From the discussion in the previous section, one can conclude that the VBCS-75 and T4FASC designs are the most promising. Both these configurations are easy to fabricate, yield a relatively high $E_{\max}$ and an acceptable spot size compared to the other configurations in Table 1. Additionally, the prepulse is dispersed with these structures.

Coincidentally, the VBCS and T4FASC configurations have been used to demonstrate that an approximately spherical TEM wave originates from the first focal point with a time spread of less than 15 ps [1, 2]. The VBCS configuration has been explored in [2]. For the T4FASC simulations in this paper, the length of the feed arms and loft connections were arbitrary, as mentioned in section 2.1.3. It is therefore necessary to optimize the feed arm and loft lengths in order to maximize $E_{\max}$ and minimize the beam width.

References

[1] Prashanth Kumar, Carl E. Baum, Serhat Altunc, Christos G. Christodoulou and Edl Schamiloglu . Near-field time-of-arrival measurements for four feed-arms with a bicone switch. EM Implosion Memo 37, February 2010.

[2] Prashanth Kumar, Carl E. Baum, Serhat Altunc, Christos G. Christodoulou and Edl Schamiloglu . Effect of the impedance of a bicone switch on the focal impulse amplitude and beam width. EM Implosion Memo 38, February 2010.

[3] E. G. Farr and C. E. Baum. Prepulse Associated with the TEM Feed of an Impulse Radiating Antenna. Sensor and Simulation Note 337, March 1992.

[4] Carl E. Baum. A Circular Conical Antenna Simulator. Sensor and Simulation Note 36, March 1967.

Appendix

Focal waveform and beam width for various switch configurations

5.1 Four feed arms

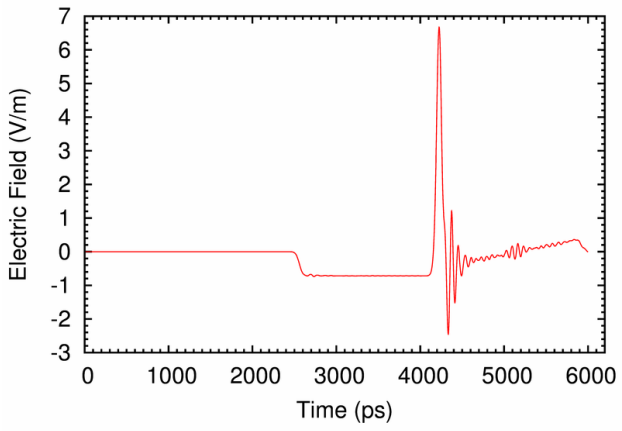

(a) Focal waveform: Four feed arms

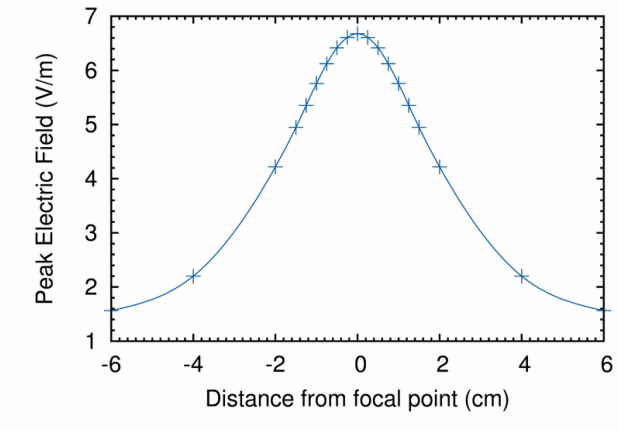

(b) Beam width: Four feed arms

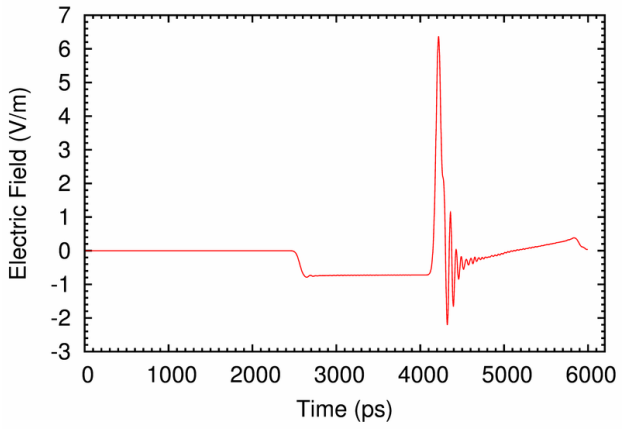

(c) Focal waveform: Four feed arms with switch cones

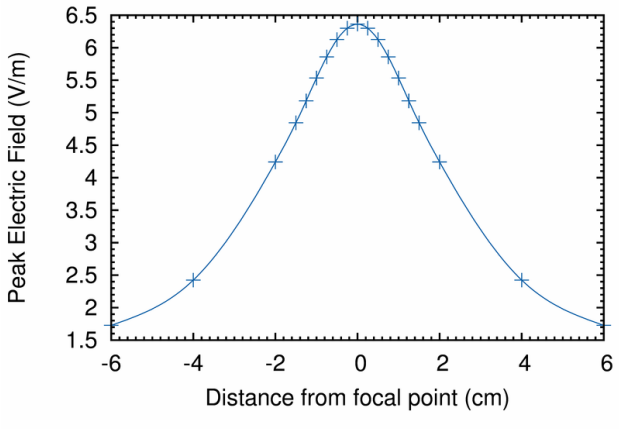

(d) Beam width: Four feed arms with switch cones

Figure 5.1: Focal impulse waveforms and beam widths for the four feed arm configurations.

5.2 Truncated four feed arms with switch cones

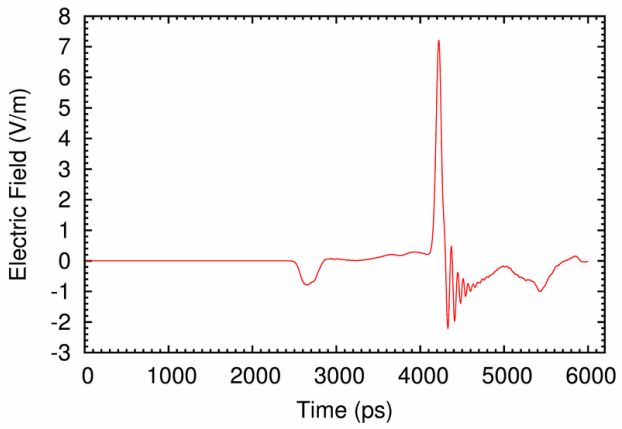

(a) Focal waveform: Truncated four feed arms with switch cones

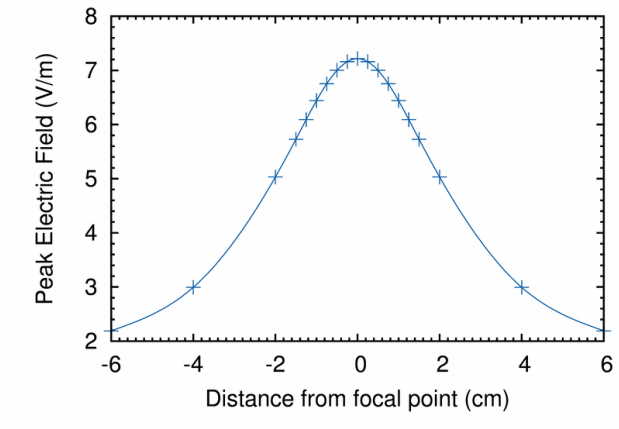

(b) Beam width: Truncated four feed arms with switch cones

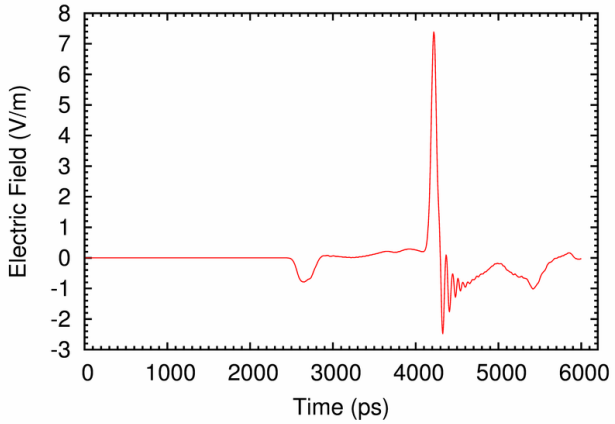

(c) Focal waveform: Truncated four feed arms with slanted switch cones

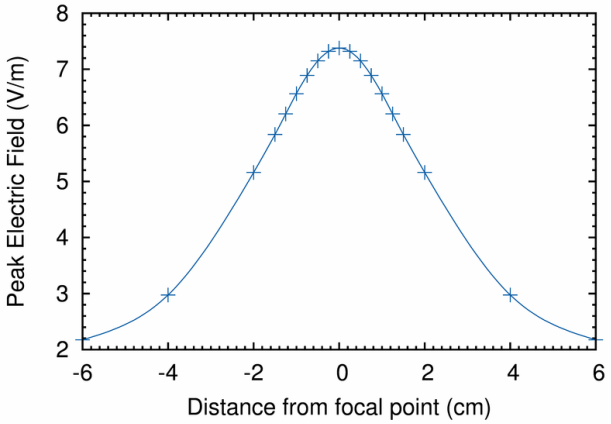

(d) Beam width: Truncated four feed arms with slanted switch cones

Figure 5.2: Focal impulse waveforms and beam widths for the truncated four feed arms with bicone switch configurations.

5.3 Slanted bicone switch

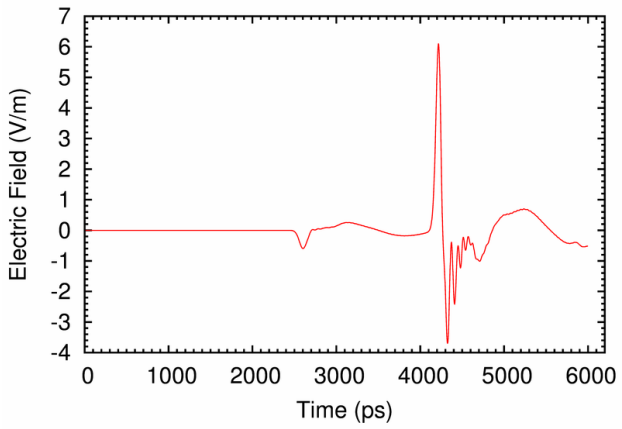

(a) Focal waveform: Truncated four feed arms with switch cones

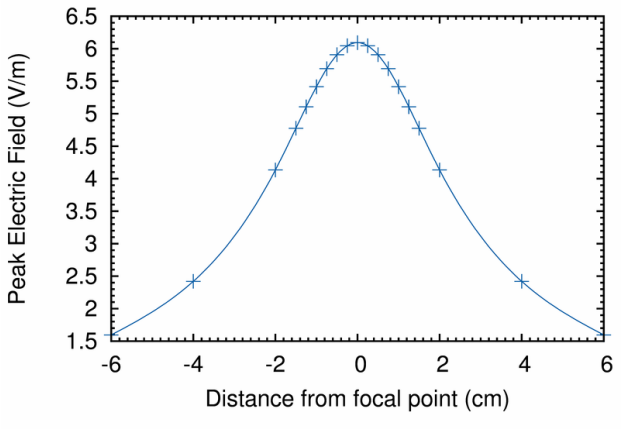

(b) Beam width: Truncated four feed arms with switch cones

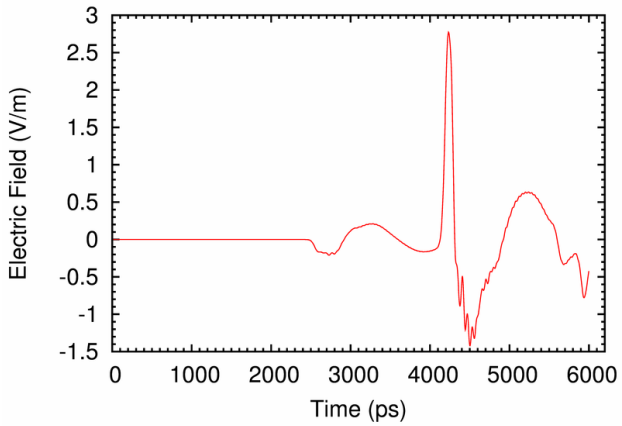

(c) Focal waveform: Truncated four feed arms with slanted switch cones

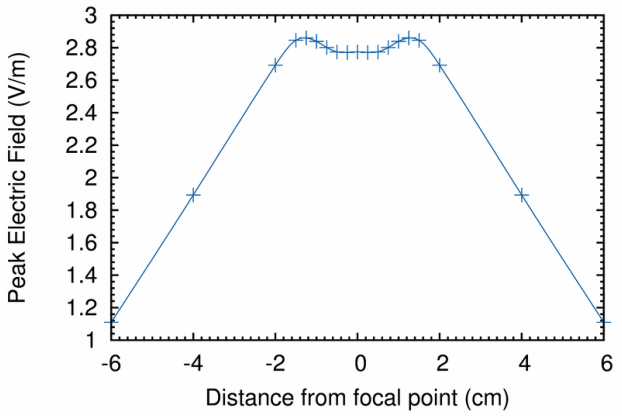

(d) Beam width: Truncated four feed arms with slanted switch cones

Figure 5.3: Focal impulse waveforms and beam widths for the slanted bicone switch configurations.

5.4 Slanted four-cone switch

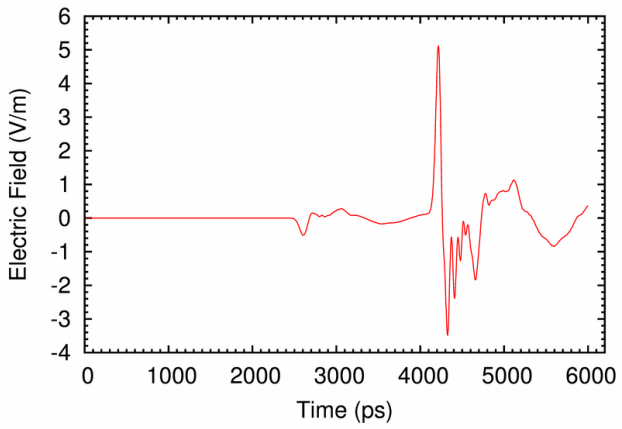

(a) Focal waveform: Truncated four feed arms with switch cones

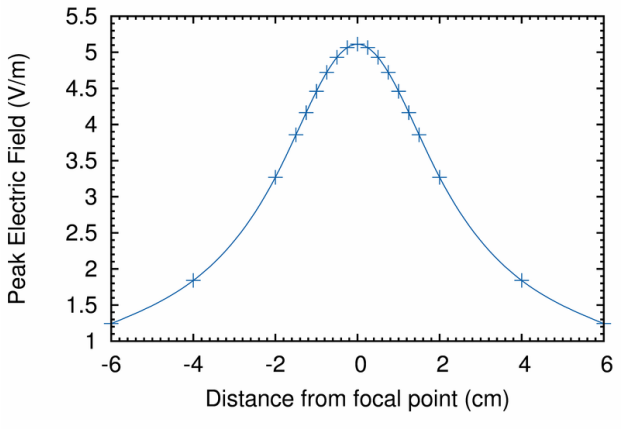

(b) Beam width: Truncated four feed arms with switch cones

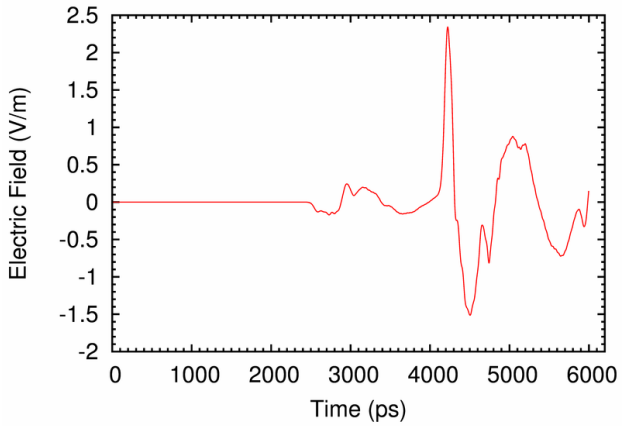

(c) Focal waveform: Truncated four feed arms with slanted switch cones

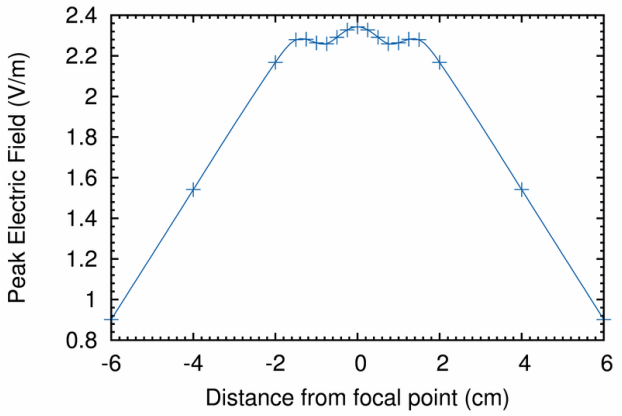

(d) Beam width: Truncated four feed arms with slanted switch cones

Figure 5.4: Focal impulse waveforms and beam widths for the slanted four-cone switch configurations.